Aerosol and Air Quality Research, 17: 2110–2118, 2017

ISSN: 1680-8584 print / 2071-1409 online
doi: 10.4209/aaqr.2017.01.0045

Ozone Catalytic Oxidation of Gaseous Toluene over MnO_2-Based Ozone Decomposition Catalysts Immobilized on a Nonwoven Fabric

Kazuhiko Sekiguchi[1*], Yuki Kurita[1], Kenshi Sankoda[1], Norikazu Namiki[2], Fumio Yasui[1,3], Hajime Tamura[3]

[1] *Graduate School of Science and Engineering, Saitama University, Sakura, Saitama 338-8570, Japan*
[2] *Faculty of Engineering, Kogakuin University, Hachioji, Tokyo 192-0015, Japan*
[3] *Techno Ryowa Ltd., Toshima, Tokyo 170-0005, Japan*

ABSTRACT

Degradation of toluene gas by ozone catalytic oxidation (OZCO) by using a MnO_2-based ozone decomposition catalyst (ODC) was investigated to clarify the reactive site of ODC material with O_3. An optimum structure for the ODC to remove O_3 and toluene were proposed. For honeycomb ODC, toluene degradation by OZCO occurred only around the entrance of the honeycomb ODC, and we expected that a thinner ODC would increase the toluene degradation efficiency. A nonwoven fabric on which ODC was immobilized was developed to decompose O_3 and volatile organic compounds simultaneously. The toluene degradation ratio and the mineralization of toluene to CO_2 were determined to evaluate the performance of the fabric. Furthermore, the effects of relative humidity and O_3 concentration on the decomposition and mineralization ratios were also investigated with or without 254 nm UV irradiation (UV_{254}). The fabric decomposed and mineralized toluene to CO_2, even at low O_3 concentrations. Although high humidity reduced the degradation ratio of toluene, UV_{254} irradiation improved the recovery of the degradation ratio and increased the mineralization ratio.

Keywords: Ozone decomposition catalyst (ODC); Ozone catalytic oxidation (OZCO); Toluene gas; Nonwoven fabric; UV irradiation.

INTRODUCTION

Ozone (O_3) is a very strong oxidant and has attracted great interest for degrading organic pollutants, such as dyes (Wu *et al.*, 2008a; Cuiping *et al.*, 2009; Srinivasan *et al.*, 2009) and other organic compounds (Perkowski *et al.*, 1996; Yan *et al.*, 2016), in wastewater, and it has been used in pilot-scale wastewater pre-treatment (Lucasa *et al.*, 2010; Somensi *et al.*, 2010). However, the reaction efficiency for ozonation alone is low (Gong *et al.*, 2008; Cuiping *et al.*, 2009; Rao and Chu, 2009) because the reactivity of O_3 depends on the chemical structure and hydrophilicity or hydrophobicity of pollutants, and the pH of the wastewater (Chang *et al.*, 2012). Therefore, O_3 is generally used in the advanced oxidation process (AOP) involving hydroxyl radicals ($OH\cdot$) combined with other oxidation techniques, such as UV and hydrogen peroxide, including the peroxone process (Hernandez *et al.*, 2002; Garoma and Gurol, 2004; Lee *et al.*, 2007; Wu *et al.*, 2008b; Cuiping *et al.*, 2009; Wang *et al.*, 2009), and electro-peroxone treatment (Wang *et al.*, 2015; Frangos *et al.*, 2016), zero-valent metals (Chand *et al.*, 2009; Wen *et al.*, 2014; Zhang *et al.*, 2015a; Zhang *et al.*, 2015b), photocatalysis (Domínguez *et al.*, 2005; Giri *et al.*, 2008; Mehrjouei *et al.*, 2015), and ultrasonication (Chand *et al.*, 2009; Joseph *et al.*, 2009). Concentrations of O_3 from several to several hundred parts per million by volume are used for AOP techniques in contamination control of gaseous pollutants and wastewater. Especially, O_3 with UV irradiation is widely used for AOP techniques because the initial cost is lower than for other oxidative degradation techniques except for ozonation alone (Mahamuni and Adewuyi, 2010). On the other hand, it has been reported that O atoms, O_2, and OH radicals are formed from O_3 on the surface of an MnO_2-based ozone decomposition catalyst (ODC) as follows (Einaga and Ogata, 2009; Zhao *et al.*, 2012; Huang *et al.*, 2015a).

$$O_3 + * \rightarrow O_2 + O* \quad (1)$$

$$O* + O_3 \rightarrow O_2 + O_2* \quad (2)$$

$$O_2* \rightarrow O_2 + * \quad (3)$$

$$O* + H_2O \rightarrow 2OH\cdot \quad (4)$$

* Corresponding author.
Tel.: +81-48-858-9192; Fax: +81-48-858-9192
E-mail address: kseki@mail.saitama-u.ac.jp

Here, * indicates the species at the catalytic active sites. These radicals can react with volatile organic compounds (VOCs) on the ODC surface and the VOCs are decomposed and mineralized to CO and CO_2. These reactions are generally called ozone catalytic oxidation (OZCO) and are used to degrade various VOC pollutants in gaseous and aqueous phases (Villasenor *et al.*, 2002; Zhao *et al.*, 2008; Nawrocki, 2013; Jia *et al.*, 2016). In gaseous phases, a high concentration of O_3 is used, and surplus O_3 is released from the reactor outlet to the ambient air as exhaust O_3. Therefore, surplus O_3 used for contamination control must be decreased and kept within safe levels because long-term exposure to O_3 is harmful to human health even at low concentrations. The removal of O_3 is proportional to the amount of ODC; thus, granulated or honeycomb ODC is often used in large quantities for the complete removal of O_3. However, to ensure the effective use of the ODC, the part of the ODC surface to which O_3 and VOCs are adsorbed and where the decomposition process occurs should be determined to clarify the optimum structure and amount of ODC materials to install in reactors.

Furthermore, at high relative humidity (RH) in the gas phase, the removal ratio of VOC gas on the ODC surface by OZCO decreases owing to the inhibition of the adsorption of hydrophobic O_3 and VOC gas by water molecules on the ODC surface (Sekiguchi *et al.*, 2003; Jeong *et al.*, 2005). This problem has been addressed by using ODCs mixed with alumina or zeolite, which are functional adsorbents, to increase the contact between O_3 and the ODC surface (Einaga and Futamura, 2004; Einaga and Futamura, 2006; Einaga *et al.*, 2013; Rezaei *et al.*, 2013; Huang *et al.*, 2015a, b). Using these adsorbents for OZCO allows VOCs to be decomposed and mineralized to CO and CO_2, even under wet conditions (Einaga and Futamura, 2006; Einaga *et al.*, 2013), but only a small percentage of VOCs reacted. UV irradiation of ODC powder increases the amount of VOCs decomposed CO_2 by OZCO (Sekiguchi *et al.*, 2003; Huang *et al.*, 2016). This is because UV irradiation generates OH radicals effectively from O_3, which is concentrated around the ODC surface, according to the following equations (Reisz *et al.*, 2003; Cuiping *et al.*, 2009).

$$O_3 + h\nu\ (< 310\ \text{nm}) \rightarrow O(^1D) + O_2 \quad (5)$$

$$O(^1D) + H_2O \rightarrow H_2O_2 \quad (6)$$

$$H_2O_2 + h\nu \rightarrow 2OH\cdot \quad (7)$$

OH radical generation from H_2O_2 depends on the light intensity (Rosenfeldt *et al.*, 2006); however, because ODC usually has a granular or honeycomb structure, it is difficult to irradiate it with UV sufficiently.

In this study, the reactive site of commercial honeycomb ODC was investigated by using a laboratory-scale single- or three-step reactor. Based on these results, a thin, flexible ODC material, fabricated from an ODC immobilized on a nonwoven fabric (nonwoven ODC), was developed and the use of the ODC was evaluated. The performance of the nonwoven ODC, namely the decomposition ratio of O_3, decomposition ratio of toluene, and the complete mineralization ratio of toluene to CO and CO_2, were investigated by using the same reactor. Furthermore, the effects of O_3 concentration and RH on the decomposition and mineralization ratios were also investigated with or without UV irradiation.

METHODS

Experimental Setup and Procedure

Fig. 1 shows the experimental setup for testing the performance of honeycomb ODC, and VOC removal by OZCO with nonwoven ODC. Honeycomb or nonwoven ODC and an UV_{254} or $UV_{254+185}$ lamp (OFU, Sankyo Denki, 4W) were placed in a 0.9 L Pyrex reactor. The main wavelengths of UV_{254} and $UV_{254+185}$ were 254 nm and 254 nm with 3% of the output power at 185 nm, respectively. For honeycomb ODC, a single-step reactor with 30-mm-thick honeycomb ODC ($30^t \times 1^s$), or a three-step reactor prepared by joining three reactors each containing 10-mm-thick honeycomb ODC ($10^t \times 3^s$), was used with or without UV_{254} and $UV_{254+185}$ irradiation. $UV_{254+185}$ readily generates O_3 and OH radicals in the gas phase by photochemical reactions as follows (Jeong *et al.*, 2004, Chang *et al.*, 2013).

$$H_2O + h\nu\ (185\ \text{nm}) \rightarrow H + OH\cdot \quad (8)$$

$$O_2 + h\nu\ (< 243\ \text{nm}) \rightarrow O(^1D) + O(^3P) \quad (9)$$

$$O(^3P) + O_2 + M \rightarrow O_3 + M \quad (10)$$

However, a UV_{254} lamp without O_3 generation was selected as a light source in the experiment for OZCO of toluene using nonwoven ODC to evaluate the relationship between toluene decomposition and O_3 concentration. UV_{254} irradiation can decompose O_3 to form O radicals, similar to the surface reaction of the ODC. The model VOC gas was 40 ppm toluene for testing the performance of honeycomb ODC and 10 ppm toluene for evaluating toluene removal by OZCO with nonwoven ODC. The toluene concentrations were adjusted by mixing the toluene standard gas with purified air that was synthesized from dry N_2 and O_2. The RH of purified air was less than 10 ppm. For each experiment, 8 or 38 ppm of O_3 was generated by $UV_{254+185}$ (OZU, 4 W, Sankyo Denki, Tokyo, Japan) irradiation and mixed into the gas flow. When a high concentration of O_3 (730 ppm) was supplied to the reactor, O_3 was also generated with an O_3 generator (ED-OG-R3Lt, Ecodesign, Saitama, Japan) by electric discharge. The gas flow rates were 5.0 L min^{-1} for testing the performance of honeycomb ODC, and 1.0 L min^{-1} for toluene removal with nonwoven ODC. To control RH, water vapor was obtained by passing dried air through a porous polytetrafluoroethylene tube in ultrapure (Milli-Q) water at room temperature. The reaction temperature was maintained at room temperature (25 ± 1°C). The VOC removal experiment was started after the toluene gas was supplied to the reactor, and all experiments were performed at least three times.

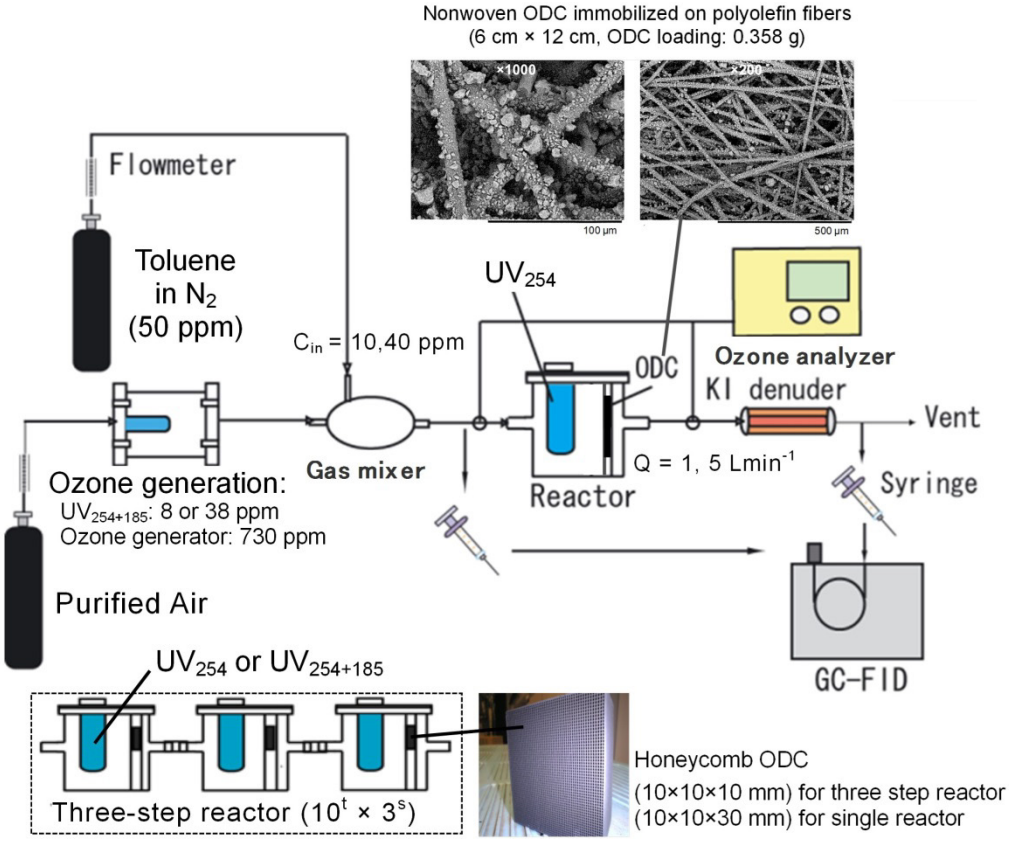

Fig. 1. Experimental setup for honeycomb ODC performance test and toluene removal by ozone catalytic oxidation with nonwoven ODC in the presence or absence of UV irradiation.

Nonwoven ODC

The ODC was a TiO_2/SiO_2 honeycomb with MnO_2 as the main active element (TSO, Nippon Syokubai, Tokyo, Japan). It was crushed with an agate pestle and mortar to a particle size of about 1.0–5.0 μm, and fixed to the nonwoven fabric fibers (Polyolefin fiber, Japan Vilene, Tokyo, Japan). The nonwoven ODC contained 0.358 g ODC in an area of 0.0072 m^2 (6 × 12 cm) and was 0.37 mm thick (Fig. 1). The surface area of the nonwoven ODC was measured with a BET surface analyzer (Flowsorb III-2305, Micromeritics, GA, USA) (Table 1). For comparison, the results for ODC powder and the TiO_2 powder (Degussa P25, Nippon Aerosil, Tokyo, Japan), widely used for photocatalytic reactions, was also described (Sekiguchi *et al.*, 2003).

The nonwoven ODC has small surface area compared with ODC powder or TiO_2 powder (Table 1). This is because ODC powder is embedded in the polyolefin fiber to immobilize it. Therefore, to use the nonwoven ODC, it is necessary to consider the saturation of VOC gas adsorption on the ODC surface (Rezaei *et al.*, 2013; Huang *et al.*, 2016). However, covering the fiber completely protects it from oxidative destruction by O_3 and active species generated from O_3 so the fabric is durable and reusable.

Analytical Method

The toluene concentration in the effluent gas was measured by gas chromatography with flame ionization detection (GC-FID; GC-390B, GL Science, Tokyo, Japan). CO_2 and CO were determined simultaneously by GC-FID (GC-15A, Shimadzu, Kyoto, Japan) equipped with a methane converter (MT-221, GL Science, Tokyo, Japan). In the experiments with O_3, a KI-coated annular denuder was used to remove the O_3 selectively, because effluent gas with a high level of O_3 can damage the GC column (Williams II and Grosjean, 1990). Low and high concentrations of O_3 were measured with a UV-absorption O_3 analyzer (UVAD-1000, Shimadzu, Kyoto, Japan) and by iodometric titration, respectively. The removal ratio and mineralization ratio were calculated by

Table 1. BET surface area of various catalysts.

Catalyst	BET surface [m^2 g^{-1}]
Nonwoven ODC	32
ODC power	113
TiO_2	51

$$\text{Removal ratio (\%)} = \frac{C_0 - C_t}{C_0} \times 100 \quad (11)$$

$$\text{Mineralization ratio (\%)} = \frac{C_{CO2,t} + C_{CO,t}}{N_C(C_0 - C_t)} \times 100 \quad (12)$$

Here, C_0 is the upstream initial concentration, C_t is the

downstream concentration after time t, $C_{CO2,t}$ and $C_{CO,t}$ are the CO_2 and CO concentrations at time t, and N_C is the carbon number of the supplied organic gas. N_C value of toluene gas is 7 (Sekiguchi *et al.*, 2010).

RESULTS AND DISCUSSION

Performance Test of Honeycomb ODC

Fig. 2 compares the toluene removal ratio using a single- or three-step reactor with or without UV irradiation for honeycomb ODC. For the single-step reactor, O_3 was completely decomposed and about 70% of the toluene gas was removed. However, the removal ratio of toluene decreased gradually with time. This result indicates that intermediate degradation products accumulated on the honeycomb ODC surface (Qi *et al.*, 2016), and active species generated from O_3 reacted with the degradation products and toluene competitively. However, UV irradiation increased the removal ratio by promoting the mineralization of degradation products (Huang *et al.*, 2016), which reactivated the ODC surface for toluene by self-cleaning. A similar self-cleaning reaction of O_3 under UV_{254} irradiation was observed for a TiO_2 surface in our previous study (Jeong *et al.*, 2004). For $UV_{254+185}$ irradiation, direct photolysis of toluene gas was also expected near the UV lamp, although the 185 nm irradiation had little effect on the toluene removal rate for short residence times in the reactor. Therefore, the increase in the toluene removal ratio by UV irradiation was caused by increasing the active species generation from O_3 by Eqs. (1)–(3) on the honeycomb ODC surface. This indicates that degradation products generated from toluene existed around the entrance of the honeycomb ODC because UV light reached only the entrance. Therefore, toluene gas was adsorbed by the whole honeycomb ODC, but O_3 decomposition, and thus toluene degradation by OZCO, only occurred only around the entrance.

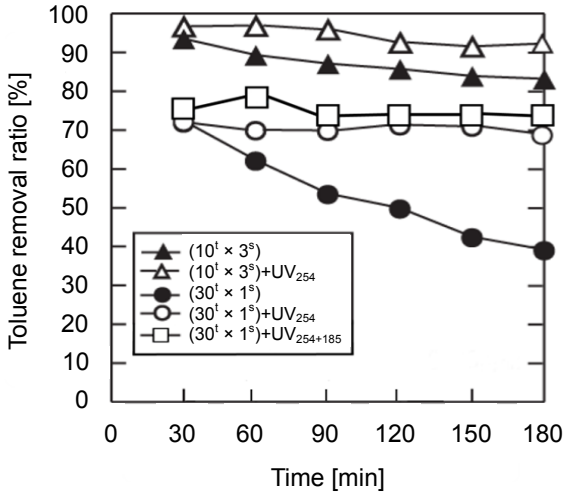

Fig. 2. Toluene removal ratio for honeycomb ODC for a single-step ($30^t \times 1^s$) or three-step ($10^t \times 3^s$) reactor with or without UV irradiation. Initial concentration of toluene: 40 ppm, initial concentration of ozone: 8 ppm, gas flow rate: 5.0 L min^{-1}, RH: < 10 ppm.

A confirmation experiment was performed with a three-step reactor (Fig. 1). The honeycomb ODC in each reactor was a third of the thickness of the honeycomb ODC used in the single reactor. In the three-step reactor, O_3 was carried to the second and third reactors without being decomposed fully by the first reactor, although the O_3 concentration decreased gradually. The three-step reactor achieved a high toluene removal ratio, especially under UV irradiation (Fig. 2). These results showed that O_3 decomposition and generation of O radicals from O_3 occurred around the entrance of the honeycomb ODC, and that degradation efficiency could be increased by using thinner ODC materials in several steps. Based on these results, we developed a thinner, flexible nonwoven ODC (0.37 mm thick) (Fig. 1). We investigated the O_3 decomposition and OZCO performance of this nonwoven ODC for toluene degradation and mineralization with or without UV irradiation under dry or wet conditions in a single-step reactor.

Effect of O_3 on Toluene Gas Removal

Fig. 3 shows the time profiles of toluene removal ratio for the nonwoven ODC with or without O_3. Without O_3, the removal ratio decreased rapidly owing to the low adsorption on the nonwoven ODC because of the small surface area. Toluene was not decomposed on the ODC surface without O_3 and was saturated immediately. However, when O_3 was supplied to the reactor, a stable removal ratio was obtained for a long time. This result indicates that even a very thin nonwoven ODC can decompose toluene effectively with the active species generated from O_3 on the ODC surface. The gas phase reaction does not contribute to the decomposition because the reaction rate of O_3 with toluene is much slower than that of active species such as OH radicals (Song *et al.*, 2007; Huangand Li, 2011).

O_3 Removal

Fig. 4 shows the removal ratios of O_3 by nonwoven ODC

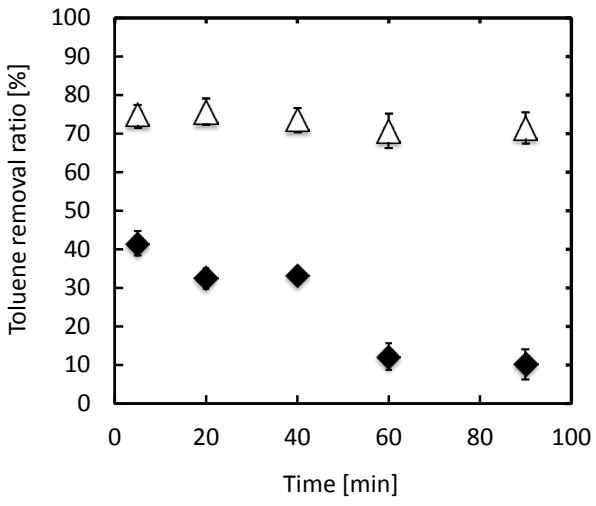

Fig. 3. Toluene removal for nonwoven ODC in the presence or absence of O_3. (◆): blank (no ozone), (△): ozone 38 ppm. Initial concentration of toluene: 10 ppm, gas flow rate: 1.0 L min^{-1}, RH: < 10 ppm.

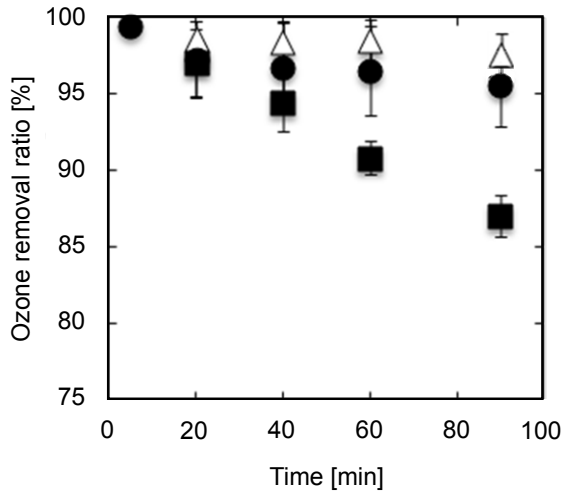

Fig. 4. Comparison of ozone removal ratio for nonwoven ODC under various conditions. (◆): ozone 38 ppm, (△): ozone 38 ppm with UV_{254} irradiation, (■): ozone 38 ppm with 70% RH. Gas flow rate: 1.0 L min^{-1}, RH: < 10 ppm except for 70% RH.

under dry and wet (RH 70%) conditions with or without UV_{254} irradiation. A removal ratio of more than 95% was maintained under dry conditions, even though the removal ratio decreased temporarily in the early stages of the reaction owing to desorption of excess O_3. Furthermore, a small increase in O_3 decomposition was observed when the nonwoven ODC was irradiated with UV_{254}, indicating that O_3 decomposition mainly occurred via the catalytic reaction of O_3 trapped on the ODC surface, not the gas phase reaction owing to the short residence time, even though UV_{254} has a wavelength of O_3 degradation (Reisz *et al.*, 2003; Cuiping *et al.*, 2009). However, the removal ratio of O_3 decreased considerably under wet (70% RH) conditions without UV_{254}, and the same trend was reported elsewhere (Sekiguchi *et al.*, 2003; Jeong *et al.*, 2005). The adsorption of hydrophobic O_3 and toluene may have been prevented by water molecules covering the ODC surface.

To clarify the O_3 degradation of the nonwoven ODC, the effect of changing the initial O_3 concentration from 38 to 730 ppm on O_3 removal ratio was measured. The O_3 removal ratio after 90 min is shown in Fig. 5. When the initial concentration of O_3 was 38 ppm, a high O_3 removal ratio of more than 95% was obtained (Fig. 4). It was thought that the amount of ODC was sufficient for 38 ppm of O_3 under these flow conditions. When the initial concentration of O_3 was changed to 730 ppm which was excessive concentration, the O_3 removal ratio decreased by 60%, although the removal ratio was stable. The amount of O_3 decomposed at 730 ppm was about 40 ppm which was similar to that at 38 ppm which was almost removed, and the concentration around 40 ppm was equivalent to the maximal decomposition amount under these flow conditions. Thus, for nonwoven ODC, the amount of removal O_3 is constant and does not depend on the O_3 concentration. Consequently, the amount of nonwoven ODC required for the O_3 removal can be determined easily.

Toluene Removal under Various Conditions

Fig. 6 shows time profiles of toluene removal ratios for nonwoven ODC under conditions of 38 ppm O_3; 38 ppm O_3 with UV_{254} irradiation; 38 ppm O_3 with 70% RH; 38 ppm O_3 with 70% RH and UV_{254} irradiation; and 730 ppm O_3. Although a stable removal ratio was obtained under all conditions, the ratio differed greatly under each set of conditions.

The removal ratio of toluene was similar under dry conditions with or without UV irradiation. Therefore, direct photolysis of toluene did not occur because a wavelength of less than 200 nm is necessary to dehydrogenate and

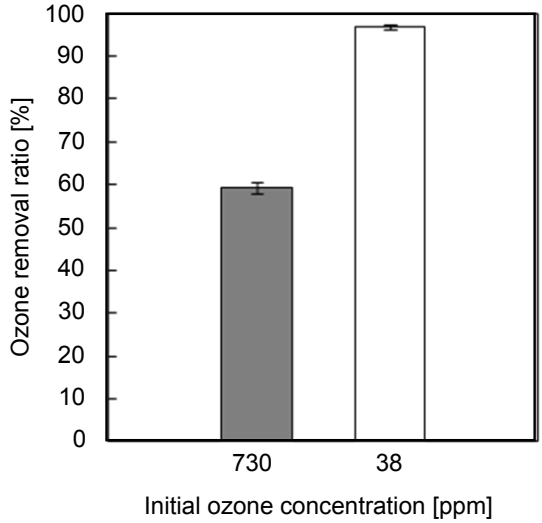

Fig. 5. Comparison of ozone removal ratio for nonwoven ODC without UV_{254} irradiation after 90 min. Gas flow rate: 1.0 L min^{-1}, RH: < 10 ppm.

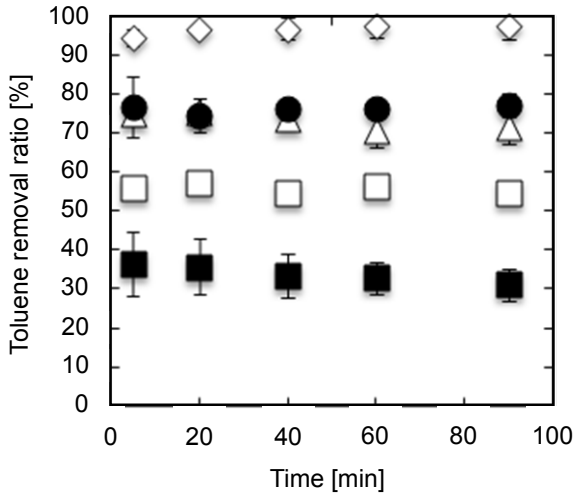

Fig. 6. Toluene removal ratios for nonwoven ODC under various conditions. (△): ozone 38 ppm, (●): ozone 38 ppm with UV_{254} irradiation, (■): ozone 38 ppm with 70% RH, (□): ozone 38 ppm with 70% RH and UV_{254} irradiation, (◇): ozone 730 ppm. Initial concentration of toluene: 10 ppm, gas flow rate: 1.0 L min^{-1}, RH: < 10 ppm except for 70% RH.

open the benzene ring (Kislov *et al.*, 2004), and toluene did not react with active species generated from O_3 in the gas phase under UV_{254} irradiation owing to the short residence time in the reactor (Wang and Ray, 2000). However, the lowest removal ratio was obtained under wet (70% RH) conditions because water molecules prevented hydrophobic toluene and O_3 from reaching the same site on the ODC surface. However, the removal ratio was stable even under wet conditions; thus, the water molecules were adsorbed on the ODC surface at a fixed rate, and toluene and the active species from O_3 reacted smoothly. The toluene removal ratio increased substantially under UV_{254} irradiation and wet conditions. This result indicated that the amount of OH radicals was increased by the generation of OH radicals by UV_{254} irradiation from O_3 concentrated near the ODC surface (Eqs. (5)–(7)), in addition to the OH radicals generated from O_3 by catalytic reactions (Eqs. (1)–(4)) on the ODC. The OH radicals generated by both processes contributed to toluene removal around the ODC surface. Therefore, nonwoven ODC generated active species and removed toluene at the ODC surface with UV_{254} irradiation even under wet conditions because the nonwoven ODC was sufficiently thin for the UV_{254} light to reach all the catalytic sites. Nonwoven ODC may be a useful material for designing multistep reactors for OZCO owing to its effective use of UV light and its thinness and flexibility.

When a high O_3 concentration (730 ppm) was supplied to the reactor, the toluene removal ratio was constant at about 100%. Because the amount of O_3 that can be decomposed at the catalyst surface is constant, the toluene removal can be explained as follows. First, ozonation in the gas phase may have occurred in a part of toluene, even during short residence times in the reactor owing to the high O_3 concentration, even though the reaction rate of O_3 with toluene is not high (Song *et al.*, 2007; Huang *et al.*, 2011), and secondary active radicals could be generated by this decomposing process to advance the toluene removal. In actual, when 730 ppm of O_3 was supplied to the reactor without ODC, the toluene removal ratio in the gas phase reaction only with O_3 was about 32.6%. Second, mineralization via the degradation of intermediate products generated by toluene decomposition at high O_3 concentrations may have increased. The active species generated from O_3 on the ODC surface may attack toluene without being affected by the degradation products. To clarify the effect of mineralization, its efficiency was evaluated under the same conditions.

Mineralization Ratio

Fig. 7 shows the toluene mineralization ratios under the same conditions as in Fig. 6. Under dry conditions without UV_{254} irradiation, the mineralization ratio was about 20%, and it increased slightly to 35% under the same conditions with UV_{254} irradiation, although both removal rates were similar to those in Fig. 6. Thus, OH radicals were generated from O_3 on the ODC surface by UV_{254} irradiation (Eqs. (5)–(7)), and contributed to the mineralization of degradation products formed by toluene decomposition. However, there was little generation of OH radicals under dry conditions, and they were competing reactions between toluene and the degradation products (Einaga and Futamura, 2004; Sekiguchi *et al.*, 2011). Under wet conditions (70% RH), the mineralization ratio increased to 50–60%, and it was much higher under UV_{254} irradiation. These results indicate that many OH radicals were generated from O_3 on the ODC surface under wet conditions (Eq. (4) without UV irradiation and Eqs. (5)–(7) with UV irradiation), and contributed to the mineralization of degradation products formed by toluene decomposition.

Under wet conditions without UV_{254} irradiation, OH radicals mainly affected mineralization; the OH radicals were not consumed by toluene decomposition owing to the low removal rate because water molecules prevented toluene adsorption. UV_{254} irradiation under wet conditions increased the removal and mineralization ratios of toluene by the OH radical reaction. Therefore, a sufficient amount of OH radicals was formed under wet conditions by UV_{254} irradiation around the ODC surface to react with both toluene and the decomposition intermediates generated from toluene.

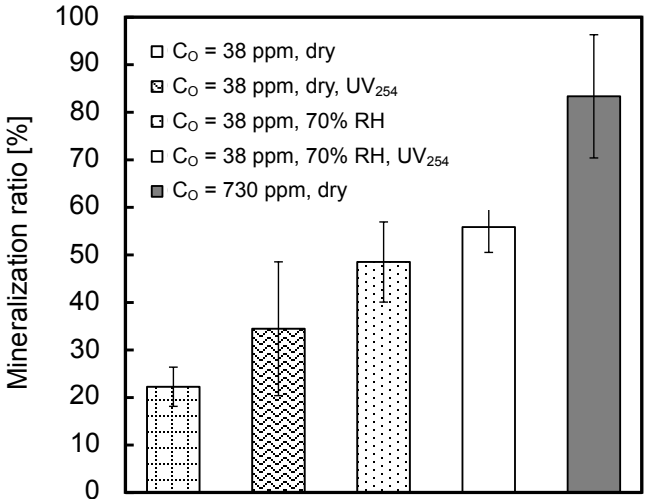

Fig. 7. Toluene mineralization ratio after 90 min under the same conditions as in Fig. 5. Initial concentration of toluene: 10 ppm, gas flow rate: 1.0 L min^{-1}, RH: < 10 ppm except for 70% RH (C_0: Initial ozone concentration).

In our previous study, the reaction rate of OH radicals formed by UV irradiation on the TiO_2 surface with intermediates was faster than that of the supplied VOC gas (Jeong *et al.*, 2005). Therefore, OH radicals generated by UV_{254} irradiation affected the mineralization of the decomposition intermediates rather than toluene removal.

When a high concentration of O_3 (730 ppm) was supplied to the reactor, the highest removal and mineralization ratios of toluene were obtained, indicating that a large amount of O radicals formed on the ODC surface via Eqs. (1)–(3), and they showed sufficient oxidization and mineralization. However, OH radicals may be generated by Eq. (4) from trace water adsorbed on the ODC surface. However, at high concentrations, O_3 acts as scavenger of OH radicals (Lee *et al.*, 2007; Cheng *et al.*, 2013), preventing the effective use of OH radicals. Based on these results, a high concentration of O_3 contributed to toluene removal and its mineralization on the nonwoven ODC surface; however, O_3 should be kept below safe levels at the reactor outlet to protect human health. Therefore, combining UV_{254} irradiation with a low concentration of O_3 that could be decomposed completely on the ODC surface resulted in effective VOC gas degradation by OZCO on the nonwoven ODC under dry or wet conditions.

CONCLUSIONS

The performance of a nonwoven ODC was investigated, focusing on the decomposition ratios of O_3 and toluene, the complete mineralization of decomposition intermediates, and the effects of RH and UV_{254} irradiation. The results of this study can be summarized as follows.

(1) O_3 was decomposed rapidly only around the entrance of the honeycomb ODC. Based on these results, a thin, flexible nonwoven ODC was developed.
(2) The amount of nonwoven ODC required for the O_3 removal can be determined easily, and toluene was decomposed and mineralized to CO_2 by OZCO, even at low O_3 concentrations.
(3) The removal ratio of toluene decreased because water molecules on the ODC surface prevented O_3 and toluene adsorption.
(4) UV_{254} irradiation of the ODC surface under wet conditions increased the removal and mineralization ratios of toluene by increasing the OH radical reaction.

Based on these results, the most effective use of nonwoven ODC for VOC gas degradation by OZCO was to combine UV irradiation with a low concentration of O_3 that can be decomposed completely on the ODC surface under dry or wet conditions. This method is promising as an air purification technique which can remove not only VOC gases but also organic particles simultaneously due to its nonwoven fabric structure.

ACKNOWLEDGMENTS

The authors thank Japan Vilene Company, Ltd. for preparing the nonwoven ODC used in our experiments. This work was supported by JSPS KAKENHI Grant Number 21246090.

REFERENCES

Chand, R., Ince, N.H., Gogate, P.R. and Bremner, D.H. (2009). Phenol degradation using 20, 300 and 520 kHz ultrasonic reactors with hydrogen peroxide, ozone and zero valent metals. *Sep. Purif. Technol.* 67: 103–109.

Chang, E.E., Liu, T.Y., Huang, C.P., Liang, C.H. and Chiang, P.C. (2012). Degradation of mefenamic acid from aqueous solutions by the ozonation and O_3/UV processes. *Sep. Purif. Technol.* 19: 123–129.

Chang, K.L., Sekiguchi, K., Wang, Q. and Zhao, F. (2013). Removal of ethylene and secondary organic aerosols using UV-$C_{254+185\ nm}$ with TiO_2 catalyst. *Aerosol Air Qual. Res.* 13: 618–626.

Cheng, Z.W., Sun, P.F., Jiang, Y.F., Yu, J.M. and Chen, J.M. (2013). Ozone-assisted $UV_{254\ nm}$ hotodegradation of gaseous ethylbenzene and chlorobenzene: Effects of process parameters, degradation pathways, and kinetic analysis. *Chem. Eng. J.* 228: 1003–1010.

Cuiping, B., Xianfeng, X., Wenqi, G., Dexin, F., Mo, X., Zhongxue, G. and Nian, X. (2011). Removal of rhodamine B by ozone-based advanced oxidation process. *Desalination* 278: 84–90.

Domínguez, J.R., Beltrán, J. and Rodríguez, O. (2005). Vis and UV photocatalytic detoxification methods (using TiO_2, TiO_2/H_2O_2, TiO_2/O_3, $TiO_2/S_2O_8^{2-}$, O_3, H_2O_2, $S_2O_8^{2-}$, Fe^{3+}/H_2O_2 and $Fe^{3+}/H_2O_2/C_2O_4^{2-}$) for dyes treatment. *Catal. Today* 101: 389–395.

Einaga, H. and Futamura, S. (2004). Catalytic oxidation of benzene with ozone over alumina-supported manganese oxides. *J. Catal.* 227: 304–312.

Einaga, H. and Futamura, S. (2006). Effect of water vapor on catalytic oxidation of benzene with ozone on alumina-supported manganese oxides. *J. Catal.* 243: 446–450.

Einaga, H. and Ogata, A. (2009). Benzene oxidation with ozone over supported manganese oxide catalysts: Effect of catalyst support and reaction conditions. *J. Hazard. Mater.* 164: 1236–1241.

Einaga, H., Teraoka, Y. and Ogata, A. (2013). Catalytic Oxidation of Benzene by Ozone over Manganese Oxides Supported on USY Zeolite. *J. Catal.* 305: 227–237.

Frangos, P., Wang, H., Shen, W., Yu, G., Deng, S., Huang, J., Wang, B. and Wang, Y. (2016). A novel photoelectro-peroxone process for the degradation and mineralization of substituted benzenes in water. *Chem. Eng. J.* 286: 239–248.

Garoma, T. and Gurol, M.D. (2004). Degradation of tert-butyl alcohol in dilute aqueous solution by an O_3/UV process. *Environ. Sci. Technol.* 38: 5246–5252.

Giri, R.R., Ozaki, H., Takanami, R. and Taniguchi, S. (2008). Heterogeneous photocatalytc ozonation of 2,4-D in dilute aqueous solution with TiO_2 fiber. *Water Sci. Technol.* 58: 207–216.

Gong, J., Liu, Y. and Sun, X. (2008). O_3 and UV/O_3 oxidation of organic constituents of biotreated municipal wastewater. *Water Res.* 42: 1238–1244.

Hernandez, R., Zappi, M., Colucci, J. and Jones, R. (2002).

Comparing the performance of various advanced oxidation processes for treatment of acetone contaminated water. *J. Hazard. Mater.* 92: 33–50.

Huang, H. and Li, W. (2011). Destruction of toluene by ozone-enhanced photocatalysis: Performance and mechanism. *Appl. Catal. B* 102: 449–453.

Huang, H., Huang, W., Xu, Y., Ye, X., Wu, M., Shao, Q., Ou, G., Peng, Z., Shi, J., Chen, J., Feng, Q., Zan, Y., Huang, H. and Hu, P. (2015a). Catalytic oxidation of gaseous benzene with ozone over zeolite-supported metal oxide nanoparticles at room temperature. *Catal. Today* 258: 627–633.

Huang, H., Ye, X., Huang, W., Chen, J., Xu, Y., Wu, M., Sha, Q., Peng, Z., Ou, G., Shi, J., Feng, X., Feng, Q., Huang, H., Hu, P. and Leung, D.Y.C. (2015b). Ozone-catalytic oxidation of gaseous benzene over MnO_2/ZSM-5 at ambient temperature: Catalytic deactivation and its suppression. *Chem. Eng. J.* 264: 24–31.

Huang, H., Huang, H., Zhan, Y., Liu, G., Wang, X., Lu, H., Xiao, L., Feng, Q. and Leung, D.Y.C. (2016). Efficient degradation of gaseous benzene by VUV photolysis combined with ozone-assisted catalytic oxidation: Performance and mechanism. *Appl. Catal. B* 186: 62–68.

Jeong, J., Sekiguchi, K. and Sakamoto, K. (2004). Photochemical and photocatalytic degradation of gaseous toluene using short-wavelength UV Irradiation with TiO_2 catalyst: Comparison of three UV sources. *Chemosphere* 57: 663–671.

Jeong, J., Sekiguchi, K., Lee, W. and Sakamoto, K. (2005). Photodegradation of gaseous volatile organic compounds (VOCs) using TiO_2 photoirradiated by an ozone-producing UV lamp: Decomposition characteristics, identification of by-products and water-soluble organic intermediates. *J. Photochem. Photobiol. A* 169: 279–287.

Jia, J., Zhang, P. and Chen, L. (2016). Catalytic decomposition of gaseous ozone over manganese dioxides with different crystal structures. *Appl. Catal. B* 189: 210–218.

Joseph, C.G., Puma, G.L., Bono, A. and Krishnaiah, D. (2009). Sonophotocatalysis in advanced oxidation process: A short review. *Ultrason. Sonochem.* 16: 583–589.

Kislov, V.V., Nguyen, T.L., Mebel, A.M., Lin, S.H. and Smith, S.C. (2004). Photodissociation of benzene under collision-free conditions: An ab initio/Rice-Ramsperger-Kassel-Marcus study. *J. Chem. Phys.* 120: 7008–7017.

Lee, C., Yoon, J. and Gunten, U.V. (2007). Oxidative Degradation of n-nitrosodimethylamine by conventional ozonation and the advanced oxidation Process ozone/hydrogen peroxide. *Water Res.* 41: 581–590.

Lucasa, M.S., Peresa, J.A. and Puma, G.L. (2010). Treatment of winery wastewater by ozone-based advanced oxidation processes (O_3, O_3/UV and O_3/UV/H_2O_2) in a pilot-scale bubble column reactor and process economics. *Sep. Purif. Technol.* 72: 235–241.

Mahamuni, N.N. and Adewuyi, Y.G. (2010). Advanced oxidation processes (AOPs) involving ultrasound for waste water treatment: A review with emphasis on cost estimation. *Ultrason. Sonochem.* 17: 990–1003.

Mehrjouei, M., Müller, S. and Möller, D. (2015). A review on photocatalytic ozonation used for the treatment of water and wastewater. *Chem. Eng. J.* 263: 209–219.

Nawrocki, J. (2013). Catalytic ozonation in water: Controversies and questions. Discussion paper. *Appl. Catal. B* 142–143: 465–471.

Perkowski, J., Kos, L. and Ledakowicz, S. (1996). Application of ozone in textile wastewater treatment. *Ozone Sci. Eng.* 18: 73–85.

Qi, F., Chu, W. and Xu, B. (2016). Comparison of phenacetin degradation in aqueous solutions by catalytic ozonation with $CuFe_2O_4$ and its precursor: Surface properties, intermediates and reaction mechanisms. *Chem. Eng. J.* 284: 28–36.

Rao, Y.F. and Chu, W. (2009). A new approach to quantify the degradation kinetics of linuron with UV, ozonation and UV/O_3 processes. *Chemosphere* 71: 1444–1449.

Reisz, E., Schmidt, W., Schuchmann, H.P. and Sonntag, C. (2003). Photolysis of ozone in aqueous solutions in the presence of tertiary butanol. *Environ. Sci. Technol.* 37: 1941–1948.

Rezaei, E., Soltan, J. and Chen, N. (2013). Catalytic oxidation of toluene by ozone over alumina supported manganese oxides: Effect of catalyst loading. *Appl. Catal. B* 136–137: 239–247.

Rosenfeldt, E.J., Linden, K.G., Canonica, S. and Gunten, U. (2006). Comparison of the efficiency of ·OH radical formation during ozonation and the advanced oxidation processes O_3/H_2O_2 and UV/H_2O_2. *Water Res.* 40: 3695–3704.

Sekiguchi, K., Sanada, A. and Sakamoto, K. (2003). Degradation of toluene with an ozone-decomposition catalyst in the presence of ozone, and the combined effect of TiO_2 addition. *Catal. Commun.* 4: 247–252.

Sekiguchi, K., Noshiroya, D., Handa, M., Yamamoto, K., Sakamoto, K. and Namiki, N. (2010). Degradation of organic gases using ultrasonic mist generated from TiO_2 suspension. *Chemosphere* 81: 33–38.

Sekiguchi, K., Sasaki, C. and Sakamoto, K. (2011). Synergistic effects of high-frequency ultrasound on photocatalytic degradation of aldehydes and their intermediates using TiO_2 suspension in water. *Ultrason. Sonochem.* 18: 158–163.

Somensi, C.A., Simionatto, E.L., Bertoli, S.L., Wisniewski Jr., A. and Radetski, C.M. (2010). Use of ozone in a pilot-scale plant for textile wastewater pre-treatment: Physico-chemical efficiency, degradation by-products identification and environmental toxicity of treated wastewater. *J. Hazard. Mater.* 175: 235–240.

Song, C., Na, K., Warren, B., Malloy, Q. and Cocker, D.R. (2007). Secondary organic aerosol formation from m-xylene in the absence of NO_x. *Environ. Sci. Technol.* 41: 7409–7416.

Srinivasan, S.V., Rema, T., Chitra, K., Balakameswari, K.S., Suthanthararajan, R., Maheswari, B.U., Ravindranath, E. and Rajamani, S. (2009). Decolourisation of leather dye by ozonation. *Desalinatio*n 235: 88–92.

Villasenor, J., Reyes, P. and Pecchi, G. (2002). Catalytic and photocatalytic ozonation of phenol on MnO_2 supported catalysts. *Catal. Today* 76: 121–131.

Wang, H., Bakheet, B., Yuan, S., Li, X., Yu, G., Murayama,

S. and Wang, Y. (2015). Kinetics and energy efficiency for the degradation of 1,4-dioxane by electro-peroxone process. *J. Hazard. Mater.* 294: 90–98.

Wang, J.H. and Ray, M.B. (2000). Application of ultraviolet photooxidation to remove organic pollutants in the gas phase. *Sep. Purif. Technol.* 19: 11–20.

Wang, K., Guo, J., Yang, M., Junji, H. and Deng, R. (2009). Decomposition of two haloacetic acids in water using UV radiation, ozone and advanced oxidation processes. *J. Hazard. Mater.* 162: 1243–1248.

Wen, G., Wang, S.J., Ma, J., Huang, T.L., Liu, Z.Q., Zhao, L. and Su, J.F. (2014). Enhanced ozonation degradation of di-*n*-butyl phthalate by zero-valent zinc in aqueous solution: Performance and mechanism. *J. Hazard. Mater.* 265: 69–78.

Williams II, E.L. and Grosjean, D. (1990). Removal of atmospheric oxidants with annular denuders. *Environ. Sci. Technol.* 24: 811–814.

Wu, J., Doan, H. and Upreti, S. (2008a). Decolorization of aqueous textile reactive dye by ozone. *Chem. Eng. J.* 142: 156–160.

Wu, J.J., Yang, J.S., Muruganandham, M. and Wu, C.C. (2008b). The oxidation study of 2-propanol using ozone-based advanced oxidation processes. *Sep. Purif. Technol.* 62: 39–46.

Yan, P., Chen, G., Ye, M., Sun, S., Ma, H. and Lin, W. (2016). Oxidation of potassium *n*-butyl xanthate with ozone: Products and pathways. *J. Cleaner Prod.* 139: 287–294.

Zhang, J., Wu, Y., Qin, C., Liu, L. and Lan, Y. (2015a). Rapid degradation of aniline in aqueous solution by ozone in the presence of zero-valent zinc. *Chemosphere* 141: 258–264.

Zhang, J., Wu, Y., Qin, C., Liu, L. and Lan, Y. (2015b). Rapid removal of *p*-chloronitrobenzene from aqueous solution by a combination of ozone with zero-valent zinc. *Sep. Purif. Technol.* 151: 318–323.

Zhao, D.Z., Shi, C., Li, X.S., Zhu, A.M. and Jang, B.W.L. (2012). Enhanced effect of water vapor on complete oxidation of formaldehyde in air with ozone over MnO_x catalysts at room temperature. *J. Hazard. Mater.* 239–240: 362–369.

Zhao, L., Ma, J., Sun, Z.Z. and Zhai, X. (2008). Catalytic ozonation for the degradation of nitrobenzene in aqueous solution by ceramic honeycomb-supported manganese. *Appl. Catal. B* 83: 256–264.

Received for review, January 19, 2017
Revised, June 22, 2017
Accepted, July 11, 2017